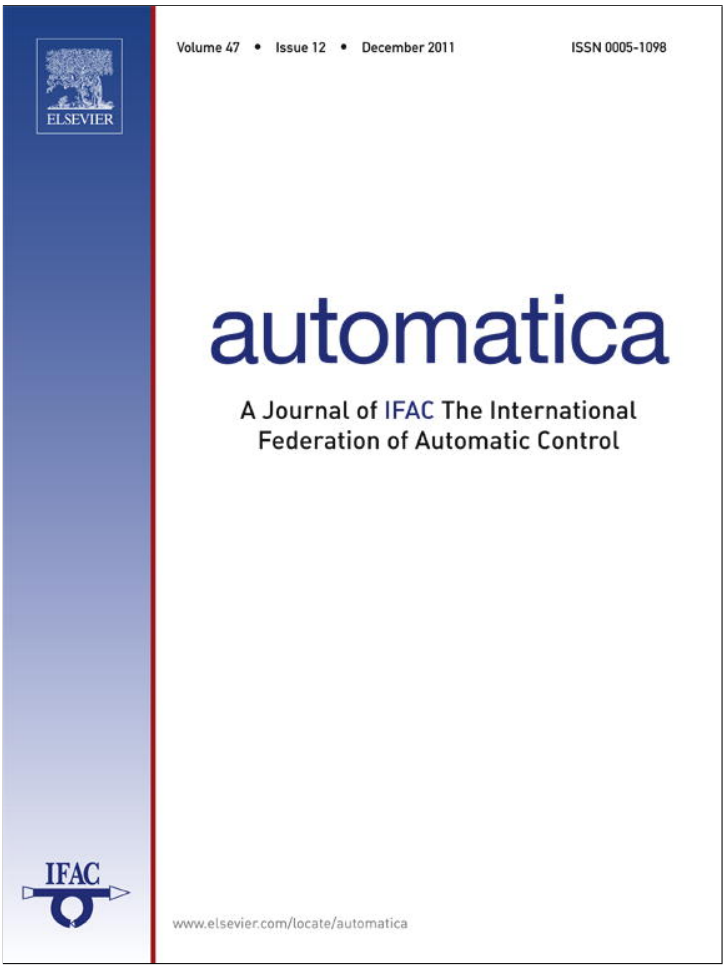

Automatica 47 (2011) 2658–2664

Contents lists available at SciVerse ScienceDirect

Automatica

journal homepage: www.elsevier.com/locate/automatica

Brief paper

Why are some hysteresis loops shaped like a butterfly?☆

Bojana Drinčić[a,1], Xiaobo Tan[b], Dennis S. Bernstein[a]

[a] Department of Aerospace Engineering, The University of Michigan, Ann Arbor, MI 48109-2140, United States

[b] Department of Electrical and Computer Engineering, Michigan State University, East Lansing, MI 48824, United States

ARTICLE INFO

Article history:
Received 20 May 2010
Received in revised form
22 April 2011
Accepted 25 April 2011
Available online 6 October 2011

Keywords:
Hysteresis
Butterfly hysteresis
Unimodal transformation
Prandtl–Ishlinskii model

ABSTRACT

The contribution of this paper is a framework for relating butterfly-shaped hysteresis maps to simple (single-loop) hysteresis maps, which are typically easier to model and more amenable to control design. In particular, a unimodal mapping is used to transform simple loops to butterfly loops. For the practically important class of piecewise monotone hysteresis maps, we provide conditions for producing butterfly-shaped maps and examine the properties of the resulting butterflies. Conversely, we present conditions under which butterfly-shaped maps can be converted to simple piecewise monotone hysteresis maps to facilitate hysteresis compensation and control design. Examples of a preloaded two-bar linkage mechanism and a magnetostrictive actuator illustrate the theory and its utility for understanding, modeling, and controlling systems with butterfly-shaped hysteresis.

1. Introduction

Hysteresis is a property of many nonlinear systems where the output-versus-input graph forms a nontrivial loop in the steady state, when the input varies periodically at an asymptotically low frequency (i.e., quasi-statically). Here a nontrivial loop means a loop with nonvanishing interior. In this paper, we refer to the aforementioned input–output loop as the *hysteresis map* of the system. The underlying mechanism that gives rise to hysteresis is multistability, which refers to the existence of multiple attracting equilibria. Under quasi-static excitation, the state of the system is attracted to different equilibria depending on the direction of the input (Bernstein, 2007).

Hysteretic systems arise in a vast range of applications, such as ferromagnetics, smart materials, biological systems, and aerodynamics (Cross, Grinfeld, & Lamba, 2009; Iyer & Tan, 2009; Leang, Zou, & Devasia, 2009; Oh, Drincic, & Bernstein, 2009; Tan & Iyer, 2009). Modeling and control of hysteresis is an area of significant interest to the controls community (Chen, Hisayama, & Su, 2009; Tan & Baras, 2004; Wang & Su, 2006; Wen & Zhou, 2007).

In some applications (e.g., a thermostat), the input–output map is independent of the frequency of excitation, and thus identical to the hysteresis map. In most applications, however, the dynamical system response depends on the frequency of excitation, and thus the input–output map is frequency-dependent and approaches the hysteresis map only as the frequency of excitation approaches zero. For details, see Oh and Bernstein (2005). In the present paper, we consider the system operating at asymptotically low frequency, ignore the transient response, and focus only on the hysteresis map, that is, on the periodic steady-state response under a quasi-static input.

The present paper focuses on butterfly-shaped hysteresis maps, which arise in many applications, such as mechanics, optics, and smart materials (Davi, 2001; Ebine & Ara, 1999; Li & Weng, 2001; Sahota, 2004). A hysteresis map is a butterfly when it consists of two loops of opposite orientation. In some applications, the shape of the hysteresis map is reminiscent of butterfly wings, which explains the terminology.

The contribution of this paper is a framework that relates butterfly-shaped hysteresis maps to simple (single-loop) hysteresis maps, which are easier to model and more amenable to control design. In particular, unimodal mappings are used to transform simple loops to butterfly loops. For piecewise monotone hysteresis maps, we provide conditions on the unimodal functions for producing butterfly-shaped maps and examine the properties of the resulting butterflies. Conversely, we present conditions under which butterfly-shaped maps can be converted to simple piecewise monotone hysteresis maps to facilitate hysteresis compensation and control design.

Although butterfly hysteresis maps are widely observed in the literature, we are not aware of any prior explanations of the

☆ This research is supported in part by a National Defense Science and Engineering Graduate Fellowship and NSF Grants 0758363 and 0824830. The material in this paper was presented at the 2009 American Control Conference (ACC 2009), June 10–12, 2009, St. Louis, Missouri, USA. This paper was recommended for publication in revised form by Associate Editor Alessandro Astolfi under the direction of Editor Andrew R. Teel.

E-mail addresses: bojanad@umich.edu (B. Drinčić), xbtan@egr.msu.edu (X. Tan), dsbaero@umich.edu (D.S. Bernstein).

[1] Tel.: +1 734 764 7573; fax: +1 734 763 0578.

0005-1098/$ – see front matter © 2011 Elsevier Ltd. All rights reserved.
doi:10.1016/j.automatica.2011.08.027

significance or origin of the characteristic shape of these maps. The proposed framework can be used to better understand and model dynamical systems involving butterfly-shaped hysteresis. To illustrate this point, we consider the preloaded two-bar linkage, which is a classical example of elastic instability (Simitses, 1967). The hysteretic nature of this mechanism is studied by Padthe, Chaturvedi, Bernstein, Bhat, and Waas (2008), where the hysteresis map is shown to be a simple closed curve in terms of the force input and linkage joint displacement output. In the present paper, we show that if we take the displacement of the spring-loaded mass as output, then the resulting hysteresis map is a butterfly. The mapping from the joint displacement to the displacement of the spring-loaded mass can be given explicitly and is clearly unimodal.

The proposed framework can also facilitate control design for systems demonstrating butterfly-shaped hysteresis maps. By transforming the butterfly map into a simple hysteresis map, we can exploit various well-studied hysteresis operators, such as the Preisach operator and the Prandtl–Ishlinskii (PI) operator (Brokate & Sprekels, 1996; Janaideh, Mao, Rakheja, Xie, & Su, 2008; Kuhnen, 2003; Mayergoyz, 2003; Tan & Baras, 2004; Visintin, 1994), and their inverses (Tan & Iyer, 2009) to develop effective hysteresis compensation and control schemes. We demonstrate this point by considering the butterfly-shaped hysteresis map for a magnetostrictive actuator (Tan, 2002). In particular, we show that a quadratic law rooted in the physics of magnetostrictive materials serves as a unimodal function for transforming the butterfly into a simple, piecewise monotone hysteresis map. The latter is then modeled with a generalized PI operator for inverse hysteresis compensation.

The contents of this paper are as follows. In Section 2, we describe a framework for mapping simple hysteresis maps into butterflies with unimodal functions, and present conditions that allow such transformations in cases involving piecewise monotone hysteresis maps. In Section 3, we consider a preloaded two-bar linkage mechanism, where the simple hysteresis loop between the linkage joint displacement and the force input is converted into a butterfly loop when a kinematics-based unimodal mapping is applied. In Section 4, the example of modeling and compensating magnetostrictive hysteresis is presented. Finally, concluding remarks are provided in Section 5. A preliminary version of some of the results of this paper is given in Drinčić and Bernstein (2009).

2. Transformation between simple and butterfly-shaped hysteresis maps

A hysteresis map is called *simple*, if it is a *simple* (oriented) closed curve, which divides the plane into three sets, namely, the interior region, the exterior region, and the curve itself (Guillemin & Pollack, 1974). Throughout this paper, let $\mathcal{C}$ be a simple hysteresis map and let $[x_0, x_1] \times [y_0, y_1]$ be the smallest rectangle with sides parallel to the x- and y-axes containing $\mathcal{C}$. We assume that, for each $x \in (x_0, x_1)$, there exists a unique pair of points $(x, y_{\min}(x)), (x, y_{\max}(x)) \in \mathcal{C}$ such that $y_{\min}(x) < y_{\max}(x)$. The following definitions are needed.

Definition 1. A continuous map $f : [y_0, y_1] \to \mathbb{R}$ is $\wedge$- unimodal if there exists $y_c \in (y_0, y_1)$ such that f is increasing on $[y_0, y_c)$ and decreasing on $(y_c, y_1]$. f is $\vee$-unimodal if there exists $y_c \in (y_0, y_1)$ such that f is decreasing on $[y_0, y_c)$ and increasing on $(y_c, y_1]$. f is unimodal if it is either $\vee$-unimodal or $\wedge$-unimodal.

Definition 2. A butterfly hysteresis map, or a butterfly, is the union of two oriented simple closed curves with disjoint interiors, a single point of intersection, and opposite orientation, such that the curves are contained in the rectangle $[x_0, x_1] \times [q_0, q_1]$ and for each $x \in (x_0, x_1)$, the intersection of the curves and the vertical line through x consists of at most two points.

For $f : [y_0, y_1] \to \mathbb{R}$, define $f(\mathcal{C}) \triangleq \{(x, f(y)) : (x, y) \in \mathcal{C}\}$. The following result is immediate.

Lemma 3. *Let $f : [y_0, y_1] \to \mathbb{R}$ be unimodal. Then $\mathcal{C}' = f(\mathcal{C})$ is a butterfly if and only if there exist disjoint open intervals $\mathcal{I}_1$ and $\mathcal{I}_2$ such that $[x_0, x_1] = \mathrm{cl}(\mathcal{I}_1) \cup \mathrm{cl}(\mathcal{I}_2)$, and such that, for all $x \in \mathcal{I}_1$ and all $x' \in \mathcal{I}_2$,*

$$[f(y_{\min}(x)) - f(y_{\max}(x))][f(y_{\min}(x')) - f(y_{\max}(x'))] < 0. \tag{1}$$

We use the notation cl to denote the closure of a set. Note that $\mathrm{cl}(\mathcal{I}_1) \cap \mathrm{cl}(\mathcal{I}_2)$ is a single point. From Lemma 3, it is straightforward to establish the following.

Corollary 4. *If a simple hysteresis map $\mathcal{C}$ is left–right symmetric or up–down symmetric, then there exists no unimodal function f, such that $\mathcal{C}' = f(\mathcal{C})$ is a butterfly.*

Next, we focus on a special class of simple hysteresis maps that are piecewise monotonic. This type of hysteresis maps is common in smart materials.

Definition 5. Let $\mathcal{C}$ be a simple hysteresis map such that, for $x = x_0$, there exists a unique point $(x_0, y) \in \mathcal{C}$ and, for $x = x_1$, there exists a unique point $(x_1, y) \in \mathcal{C}$. $\mathcal{C}$ is called piecewise monotonically decreasing if $y_{\min}(x)$ and $y_{\max}(x)$ are decreasing functions of x. $\mathcal{C}$ is piecewise monotonically increasing if $y_{\min}(x)$ and $y_{\max}(x)$ are increasing functions of x. $\mathcal{C}$ is piecewise monotonic if it is either piecewise monotonically decreasing or piecewise monotonically increasing.

The following lemma is used in the proof of Theorem 7.

Lemma 6. *Let $\mathcal{S}$ be a closed polygonal region in a plane with vertices A, B, C, D, labeled consecutively. Let $\mathcal{C}_1$ be a continuous curve that connects A to C and satisfies $\mathcal{C}_1 \setminus \{A, C\} \subset \mathrm{int}(\mathcal{S})$. Let $\mathcal{C}_2$ be a continuous curve that connects B to D and satisfies $\mathcal{C}_2 \setminus \{B, D\} \subset \mathrm{int}(\mathcal{S})$. Then $\mathcal{C}_1 \cap \mathcal{C}_2 \neq \emptyset$. If, in addition, there exist coordinate axes with respect to which $\mathcal{C}_1$ is a monotonically increasing (resp. decreasing) function and $\mathcal{C}_2$ is a monotonically decreasing (resp. increasing) function, then $\mathcal{C}_1 \cap \mathcal{C}_2$ consists of a single point.*

Proof. Because $\mathcal{C}_1$ is a continuous curve connecting A to C, it divides $\mathcal{S}$ into two open disjoint regions R_1 and R_2, where $B \in R_1$ and $D \in R_2$. Since the curve $\mathcal{C}_2$ connects points B and D it must cross from region R_1 to region R_2. From the Jordan curve lemma, $\mathcal{C}_2$ must cross the boundary between these regions, that is, the curve $\mathcal{C}_1$. It is straightforward that there exists a unique point of intersection between $\mathcal{C}_1$ and $\mathcal{C}_2$ if, with respect to some axes, these curves are monotonic with opposite monotonicity. □

Theorem 7. *Let $\mathcal{C}$ be a piecewise monotonic simple hysteresis map. Furthermore, let f be a $\vee$-unimodal function with its minimum point $q_c(y_c)$ such that $y_c \in (y_0, y_1)$ or a $\wedge$-unimodal function with its maximum point $q_c(y_c)$, such that $y_c \in (y_0, y_1)$. Then $\mathcal{C}' = f(\mathcal{C})$ is a butterfly.*

Proof. We assume that the map f is $\vee$-unimodal and that $\mathcal{C}$ is monotonically increasing; the remaining three cases are analogous. Let $\mathcal{J}_1 = (x_0, x_{c1})$, where $x_{c1} \in (x_0, x_1)$ and $y_{\max}(x_{c1}) = y_c$, and let $\mathcal{J}_2 = (x_{c2}, x_1)$, where $x_{c2} \in (x_0, x_1)$ and $y_{\min}(x_{c2}) = y_c$. Note that $x_{c1} < x_{c2}$. Because f is $\vee$-unimodal, $f(y_a) < f(y_b)$ for $y_a, y_b \in [y_0, y_c]$ such that $y_a > y_b$, and $f(y_a) > f(y_b)$ for $y_a, y_b \in [y_c, y_1]$ such that $y_a > y_b$. Thus, for all $x \in \mathcal{J}_1, f(y_{\max}(x)) < f(y_{\min}(x))$, and, for all $x \in \mathcal{J}_2, f(y_{\max}(x)) > f(y_{\min}(x))$.

Let $\mathcal{J}_3 = [x_{c1}, x_{c2}]$. Since $\mathcal{C}$ and f are piecewise monotonic, $\mathcal{C}_1 = \{(x, f(y_{\max}(x))) : x \in \mathcal{J}_3\}$ is monotonically increasing and $\mathcal{C}_2 = \{(x, f(y_{\min}(x))) : x \in \mathcal{J}_3\}$ is monotonically decreasing. Furthermore, it follows from Lemma 6 that $\mathcal{C}_1 \cap \mathcal{C}_2$ consists of a

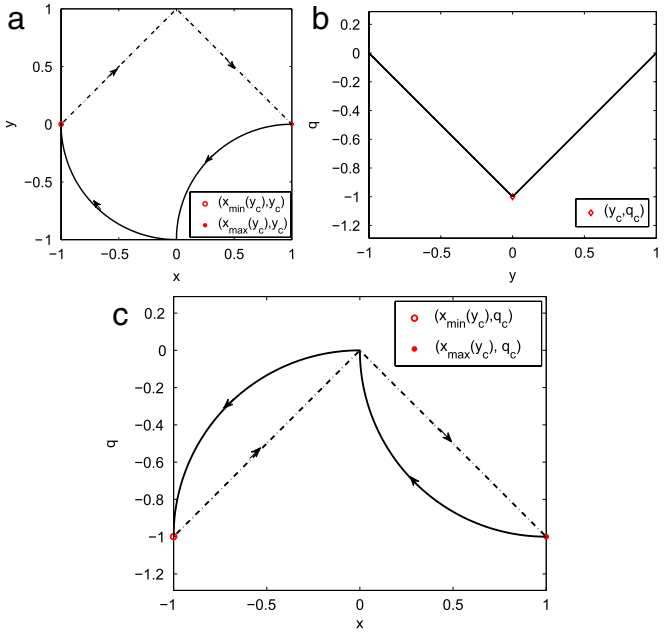

Fig. 1. Illustration of the proof of Theorem 9. The simple hysteresis map $\mathcal{C}$ and points $(x_{\min}(y_c), y_c)$ and $(x_{\max}(y_c), y_c)$ are shown in (a). The $\vee$-unimodal map f and the point (y_c, q_c) are shown in (b). The butterfly map $\mathcal{C}'$ and the points $(x_{\min}(q_c), q_c)$ and $(x_{\max}(q_c), q_c)$ are shown in (c).

unique point (x_*, q_*). Now, for all $x \in \mathcal{I}_1 = (x_0, x_*)$, $f(y_{\max}(x)) < f(y_{\min}(x))$ while, for all $x \in \mathcal{I}_2 = (x_*, x_1)$, $f(y_{\max}(x)) > f(y_{\min}(x))$. Thus, (1) is satisfied for all $x \in \mathcal{I}_1$ and all $x' \in \mathcal{I}_2$, and thus $\mathcal{C}' = f(\mathcal{C})$ is a butterfly. □

We now further investigate the properties of the butterfly map created by applying a unimodal map to a simple hysteresis map $\mathcal{C}$. The following definition is needed.

Definition 8. Let $\mathcal{C}$ be a simple hysteresis map or a butterfly, and let $[x_0, x_1] \times [y_0, y_1]$ be the smallest rectangle containing $\mathcal{C}$. A point $(x, y_0) \in \mathcal{C}$ is a minimum of $\mathcal{C}$. A point $(x, y_1) \in \mathcal{C}$ is a maximum of $\mathcal{C}$.

The following result, which is not restricted to the class of piecewise monotone simple hysteresis maps, is illustrated in Fig. 1.

Theorem 9. *Let $f : [y_0, y_1] \to \mathbb{R}$ be unimodal and let $\mathcal{C}$ be a simple hysteresis map defined on the rectangle $[x_0, x_1] \times [y_0, y_1]$. Assume that, for each $y \in (y_0, y_1)$, there exists a unique pair of points $(x_{\min}(y), y)$, $(x_{\max}(y), y) \in \mathcal{C}$ such that $x_{\min}(y) < x_{\max}(y)$, and assume that $\mathcal{C}' \triangleq f(\mathcal{C})$ is a butterfly. If f is $\vee$-unimodal, then $\mathcal{C}'$ has exactly two minima, which are equal. Alternatively, if f is $\wedge$-unimodal, then $\mathcal{C}'$ has exactly two maxima, which are equal.*

Proof. We assume that the map f is $\vee$-unimodal; the $\wedge$-unimodal case is analogous. Let $[x_0, x_1] \times [q_c, q_1]$ be the smallest rectangle containing $\mathcal{C}'$. Let $y_c \in (y_0, y_1)$ satisfy $q_c = f(y_c)$. By Definition 1, y_c is the global minimizer of f. By assumption, there exist exactly two points $(x_{\min}(y_c), y_c)$ and $(x_{\max}(y_c), y_c) \in \mathcal{C}$ such that $x_{\min}(y_c) < x_{\max}(y_c)$. Applying f to these points yields $(x_{\min}(y_c), f(y_c))$, $(x_{\max}(y_c), f(y_c)) \in \mathcal{C}'$. Hence these points are the minima of the curve $\mathcal{C}'$ and, since $x_{\min}(y_c) \neq x_{\max}(y_c)$, it follows that these points are distinct. Thus, the butterfly map $\mathcal{C}'$ has exactly two minima of equal value q_c. □

The following theorem is related to Theorem 9 and represents the dual of Theorem 7, and informs when a butterfly can be transformed into a simple, piecewise monotone hysteresis map.

Theorem 10. *Let $\mathcal{C}'$ be a butterfly and let $[x_0, x_1] \times [q_0, q_1]$ be the smallest rectangle containing $\mathcal{C}'$, with sides parallel to the x- and y-axes. Decompose $\mathcal{C}'$ as the union of two branches, namely, branch $\mathcal{B}_+$ associated with increasing x and branch $\mathcal{B}_-$ associated with decreasing x. Furthermore, define $g_+ : [x_0, x_1] \to [q_0, q_1]$ and $g_- : [x_0, x_1] \to [q_0, q_1]$, such that $\mathcal{B}_+$ and $\mathcal{B}_-$ are the graphs of g_+ and g_-, respectively.*

(a) Assume that $\mathcal{C}'$ has exactly two minima (x_a, q_c), (x_b, q_c), with $x_0 < x_a < x_b < x_1$ and $q_c = q_0$. Furthermore, assume that g_+ (resp., g_-) is decreasing on $[x_0, x_b]$ and increasing on $[x_b, x_1]$, and g_- (resp., g_+) is decreasing on $[x_0, x_a]$ and increasing on $[x_a, x_1]$. Then, for each $\vee$-unimodal function f with minimum value q_c, there exist a piecewise monotonically increasing simple hysteresis map $\mathcal{C}_1$ with counterclockwise (resp., clockwise) orientation and a piecewise monotonically decreasing simple hysteresis map $\mathcal{C}_2$ with clockwise (resp., counterclockwise) orientation, such that $\mathcal{C}' = f(\mathcal{C}_1) = f(\mathcal{C}_2)$.

(b) Assume that $\mathcal{C}'$ has exactly two maxima (x_a, q_c), (x_b, q_c), with $x_0 < x_a < x_b < x_1$ and $q_c = q_1$. Furthermore, assume that g_+ (resp., g_-) is increasing on $[x_0, x_b]$ and decreasing on $[x_b, x_1]$, and g_- (resp., g_+) is increasing on $[x_0, x_a]$ and decreasing on $[x_a, x_1]$. Then, for each $\wedge$-unimodal function f with maximum value q_c, there exist a piecewise monotonically increasing simple hysteresis map $\mathcal{C}_1$ with counterclockwise (resp., clockwise) orientation and a piecewise monotonically decreasing simple hysteresis map $\mathcal{C}_2$ with clockwise (resp., counterclockwise) orientation, such that $\mathcal{C}' = f(\mathcal{C}_1) = f(\mathcal{C}_2)$.

Proof. We prove the case in (a) where g_+ is decreasing on $[x_0, x_b]$ and increasing on $[x_b, x_1]$, and g_- is decreasing on $[x_0, x_a]$ and increasing on $[x_a, x_1]$, as illustrated in Fig. 2(a). The other case in (a) and the two cases in (b) can be proven analogously. Let f be a $\vee$-unimodal function, such that $f(y_c) = q_c$ for some y_c, and

$$f(y) = \begin{cases} f_-(y), & \text{if } y \leq y_c, \\ f_+(y), & \text{if } y \geq y_c, \end{cases}$$

where the continuous functions f_- and f_+ are strictly decreasing and increasing, respectively (Fig. 2(b)). Let f_-^{-1} and f_+^{-1} denote the inverse functions of f_- and f_+, respectively, as illustrated in Fig. 2(c). Note that f_-^{-1} is continuous and strictly decreasing, and f_+^{-1} is continuous and strictly increasing, with $y_c = f_-^{-1}(q_c) = f_+^{-1}(q_c)$. Define a curve $\mathcal{C}_1$ on the plane as the union of four directed segments that are the corresponding graphs of

$$y = f_-^{-1}(g_+(x)) \quad \text{as } x \text{ increases from } x_0 \text{ to } x_b, \tag{2}$$

$$y = f_+^{-1}(g_+(x)) \quad \text{as } x \text{ increases from } x_b \text{ to } x_1, \tag{3}$$

$$y = f_+^{-1}(g_-(x)) \quad \text{as } x \text{ decreases from } x_1 \text{ to } x_a, \tag{4}$$

$$y = f_-^{-1}(g_-(x)) \quad \text{as } x \text{ decreases from } x_a \text{ to } x_0, \tag{5}$$

as illustrated in Fig. 2(d). Since $f_-^{-1}(g_+(x_b)) = f_-^{-1}(q_c) = y_c = f_+^{-1}(g_+(x_b))$, $f_+^{-1}(g_+(x_1)) = f_+^{-1}(g_-(x_1))$ (from continuity of $\mathcal{C}'$), $f_+^{-1}(g_-(x_a)) = y_c = f_-^{-1}(g_-(x_a))$, and $f_-^{-1}(g_-(x_0)) = f_-^{-1}(g_+(x_0))$ (from continuity of $\mathcal{C}'$), $\mathcal{C}_1$ is continuous and closed.

Define $y = h_+(x)$ on $[x_0, x_1]$ using (2) and (3), and define $y = h_-(x)$ on $[x_0, x_1]$ using (4) and (5). Namely, h_+ and h_- represent the two branches of $\mathcal{C}_1$ associated with increasing and decreasing x, respectively. Using the properties of $f_\pm^{-1}$ and $g_\pm$, it can be shown that both h_+ and h_- are strictly increasing functions of x. Furthermore, for each $x \in (x_0, x_1)$, $h_+(x) < h_-(x)$. Therefore, $\mathcal{C}_1$ is a simple hysteresis map with counterclockwise orientation. Finally, $f(\mathcal{C}_1)$ can be defined as

$$f_-(y) = f_-(f_-^{-1}(g_+(x))) = g_+(x) \quad \text{as } x \text{ increases from } x_0 \text{ to } x_b, \tag{6}$$

$$f_+(y) = f_+(f_+^{-1}(g_+(x))) = g_+(x) \quad \text{as } x \text{ increases from } x_b \text{ to } x_1, \tag{7}$$

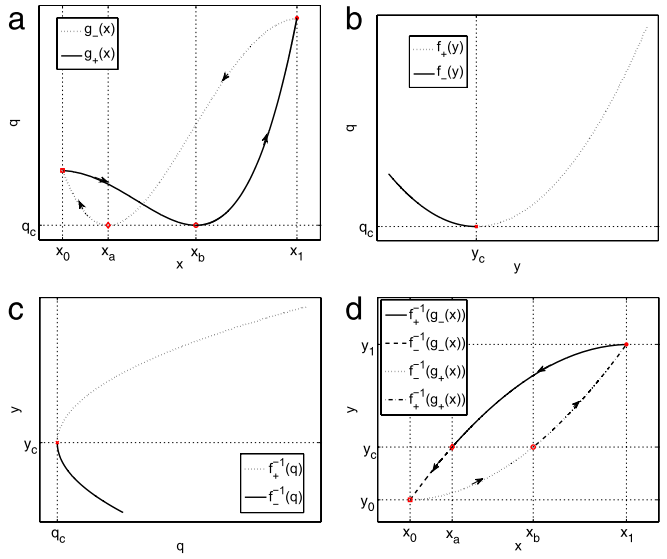

Fig. 2. Illustration of the proof of Theorem 10. A butterfly $\mathcal{C}'$ is shown in (a), and a $\vee$-unimodal function f is shown in (b). The inverse functions of f_+ and f_- in (b) are shown in (c). The constructed simple hysteresis map $\mathcal{C}$ is shown in (d).

$$f_+(y) = f_+(f_+^{-1}(g_-(x))) = g_-(x) \quad \text{as } x \text{ decreases from } x_1 \text{ to } x_a, \quad (8)$$

$$f_-(y) = f_-(f_-^{-1}(g_-(x))) = g_-(x) \quad \text{as } x \text{ decreases from } x_a \text{ to } x_0, \quad (9)$$

and, thus, $\mathcal{C}' = f(\mathcal{C}_1)$.

Following the same line of reasoning as above, it can be proven that $\mathcal{C}_2$ is a piecewise monotonically decreasing, simple hysteresis map with clockwise orientation, and $\mathcal{C}' = f(\mathcal{C}_2)$. □

In Sections 3 and 4, we show physical examples where the butterfly hysteresis loops satisfy the assumptions of Theorem 10, and the unimodal functions linking the butterfly and simple loops are given by the physical models. If a butterfly hysteresis loop satisfies the assumptions of Theorem 10, and yet a proper physical model is not available, we can choose an arbitrary $\vee$-unimodal ($\wedge$-unimodal, resp.) function f with a minimum (maximum, resp.) value of q_c as shown. Such an f guarantees successful transformation of the butterfly loop into a simple, piecewise monotone loop. The proof of Theorem 10 is constructive, and thus it not only establishes the claims, but also illustrates how the simple loop is constructed with the chosen f. To illustrate, we transform the butterfly loop shown in Fig. 3(a) into a simple loop using the two $\vee$-unimodal functions shown in Fig. 3(b). The resulting simple loops are shown in Fig. 3(c). Note that functions f_1 and f_2 have the same minimum value q_c, but at two different values of y, namely y_c and $y_{c'}$.

3. Hysteresis in a preloaded two-bar linkage mechanism

In this section, we analyze the dynamics of a two-bar linkage with joints P, Q, and R and preloaded by a spring with stiffness constant k as shown in Fig. 4. The purpose of this discussion is to show that we can transform a simple hysteresis map into a butterfly through a unimodal map. Additional details of derivations related to the simple hysteresis map are given by Padthe et al. (2008).

A constant vertical force F is applied at Q, where the two bars are joined by a frictionless pin. Let θ denote the counterclockwise angle that the left bar makes with the horizontal, and let q denote the distance between the joints P and R. When $F = 0$, the linkage has three equilibrium configurations. In the first two, θ and q are $\pm\theta_0$ and $q_0 = 2l\cos\theta_0$, respectively, and the spring k is relaxed. For the third equilibrium, both bars are horizontal with $\theta = 0$.

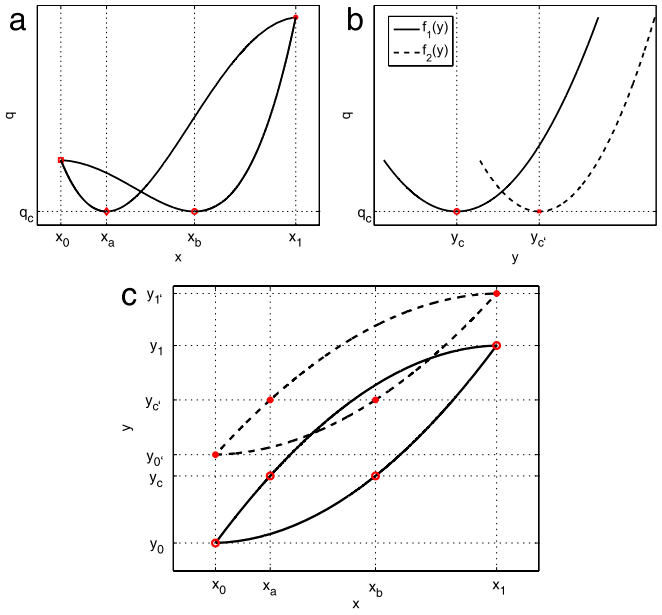

Fig. 3. Transformation of a butterfly loop into a simple loop by using two different $\vee$-unimodal functions. (a) shows the butterfly loop, (b) shows the $\vee$-unimodal functions $f_1(y) = \frac{1}{3}(y+0.5)^2 - 0.5$ (solid) and $f_2(y) = 0.5(y+0.5)^2 - 0.7$ (dashed). Applying the two different $\vee$-unimodal functions f_1^{-1} (solid) and f_2^{-1} (dashed) to the butterfly loop yields the two distinct simple butterfly loops shown in (c).

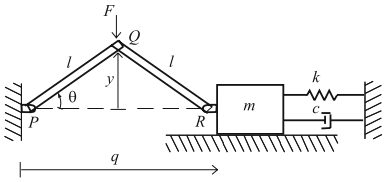

Fig. 4. A preloaded two-bar linkage with a vertical force F acting at the joint Q. The word 'preloaded' refers to the presence of the spring with stiffness constant k, which is compressed when the two-bar linkage is in the horizontal equilibrium.

Note that y is the vertical distance from the joint Q to the horizontal equilibrium, and q is the horizontal distance from joint P to joint R as shown in Fig. 4. If θ is known, then y and q can be determined from

$$y = l\sin\theta, \qquad q = 2l\cos\theta, \quad (10)$$

respectively.

The equations of motion for the preloaded two-bar linkage are given by

$$\begin{aligned}&\left(\left(2ml^2 + \frac{9}{8}m_{bar}l^2\right)\sin^2\theta + \frac{5}{24}m_{bar}l^2\right)\ddot{\theta}\\ &+ \left(2ml^2 + \frac{9}{8}m_{bar}l^2\right)(\sin\theta)(\cos\theta)\dot{\theta}^2\\ &+ 2kl^2(\cos\theta_0 - \cos\theta)(\sin\theta)\\ &+ 2cl^2(\sin\theta)^2\dot{\theta} = -\frac{l\cos\theta}{2}F, \end{aligned} \quad (11)$$

where m_{bar} is the inertia of each bar. Using (10), the nonlinear dynamics (11) can be expressed in terms of the displacement q or y.

We use (11) and (10) to simulate the linkage dynamics under the periodic external force $F = \sin(0.001t)$ N with parameter values $k = 1$ N/m, $m = 1$ kg, $c = 1$ N − s/m, $m_{bar} = 0.5$ kg, and $l = 1$ m. As shown in Fig. 5(a), there exists a nontrivial clockwise hysteresis map from the vertical force F to the vertical displacement y at low frequencies. The presence of a nontrivial loop at asymptotically low frequencies constitutes

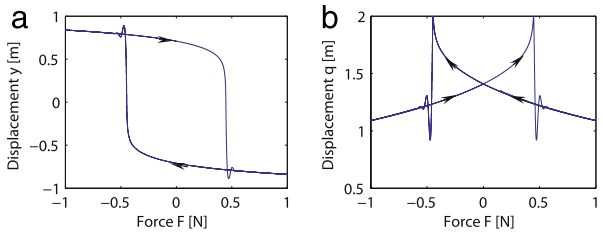

Fig. 5. Input–output maps of the two-bar linkage model (11) for $F = \sin(0.001t)$. (a) shows the hysteresis map with the output variable y, while (b) shows the butterfly hysteresis map with the output variable q. The parameter values are $k = 1$ N/m, $m = 1$ kg, $c = 1$ N $-$ s/m, $m_{bar} = 0.5$ kg, and $l = 1$ m.

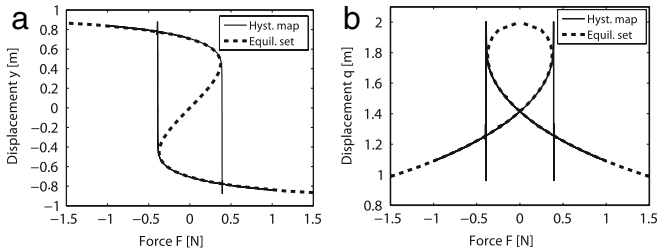

Fig. 6. Comparison of the equilibrium sets $\mathcal{E}$ and the hysteresis maps for the preloaded two-bar linkage. The output variable is y in (a) and q in (b). The hysteresis map is a subset of $\mathcal{E}$ except for the vertical segments at the bifurcation points. The parameter values are given in Fig. 5(a) with $F(t) = \sin(0.001t)$ N.

hysteresis. Fig. 5(b) shows the input–output map between the vertical force F and horizontal displacement q. At asymptotically low frequencies this input–output map is a symmetric butterfly with two loops of opposite orientation.

The equilibrium set $\mathcal{E}$ for the preloaded two-bar linkage is the set of points (F, y) that satisfy

$$y\left(1 - \frac{l\cos\theta_0}{\sqrt{l^2 - y^2}}\right) = \frac{F}{4k}. \tag{12}$$

Alternatively, the set $\mathcal{E}$ can be expressed as the set of points (F, q) that satisfy

$$\pm\sqrt{(4l^2 - q^2)}\left(1 - \frac{2l\cos\theta_0}{q}\right) = \frac{F}{2k}. \tag{13}$$

The equilibrium sets $\mathcal{E}$ defined by (12)–(13) are shown in Fig. 6. The corresponding hysteresis maps (as the force varies quasi-statically) are also shown in Fig. 6. The set $\mathcal{E}$ is useful for analyzing the hysteresis of the preloaded two-bar linkage. It is shown in Oh and Bernstein (2005) that a system that exhibits hysteresis has a multi-valued equilibrium map and that the hysteresis map is a subset of the equilibrium map. The only parts of the hysteresis map that do not belong to the equilibria set are the vertical sections.

Thus the hysteresis map is a simple closed curve when the output variable is y and a butterfly when the output variable is q. Furthermore, we note that the butterfly in Fig. 5(b) satisfies the conditions of Theorem 10(b), which implies that f should be $\wedge$-unimodal. From the kinematics equation (10) we find the unimodal map $f = \sqrt{4(l^2 - y^2)}$ shown in Fig. 7, which is indeed $\wedge$-unimodal and transforms the simple hysteresis map into a butterfly.

4. Hysteresis in a magnetostrictive actuator

In this section, we present butterfly hysteresis data obtained from a magnetostrictive actuator. Based on material physics, we find the unimodal function that relates the butterfly hysteresis map to a simple hysteresis map that is piecewise monotone.

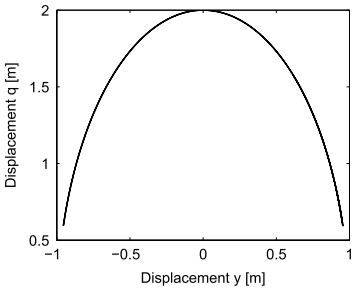

Fig. 7. The $\wedge$-unimodal mapping function $f(y) = \sqrt{4(l^2 - y^2)}$, which transforms the simple hysteresis map of the buckling mechanism into a butterfly.

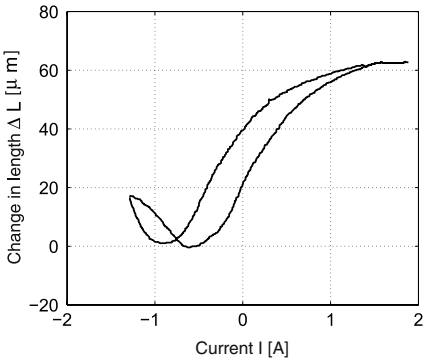

Fig. 8. Experimental displacement-to-current butterfly hysteresis in a Terfenol-D magnetostrictive actuator (Tan, 2002).

The latter can be modeled with a hysteresis operator such as generalized Prandtl–Ishlinskii model, which can then be inverted for compensation of the hysteresis effect in the magnetostrictive actuator.

A Terfenol-D magnetostrictive actuator manufactured by Etrema Products, Inc. exhibits displacement-to-current butterfly hysteresis shown in Fig. 8. We note that the observed butterfly has two minima that are approximately equal, and can be taken as satisfying assumptions of Theorem 10. In order to transform the butterfly into a simple hysteresis map, we adopt the following from Tan (2002).

Definition 11. Let ΔL be the change in the length of the magnetostrictive rod, and let L_{rod} be the length of the demagnetized rod. Then the magnetostriction in the rod is

$$\lambda \triangleq \frac{\Delta L}{L_{\text{rod}}}. \tag{14}$$

Based on the physics of magnetostrictive materials (Brown, 1966) the magnetostriction λ and the magnetization M along the rod direction can be approximately related through a quadratic law stated in Tan (2002)

$$\lambda = a_1 M^2 + b_1, \tag{15}$$

where $a_1 = \frac{\lambda_s}{M_s^2}$, b_1 is a constant, λ_s is the saturation magnetostriction, and M_s is the saturation magnetization. The input current I and the magnetic field H are related through

$$H = c_0 I + H_{\text{bias}}, \tag{16}$$

where c_0 is the coil factor and H_{bias} is the bias field produced by a dc current. Actuator specifications state that $M_s = 7.87 \times 10^5$ A/m, $L_{\text{rod}} = 5.13 \times 10^{-2}$ m, $c_0 = 1.54 \times 10^4$ m^{-1}; the remaining parameters are experimentally identified to be $\lambda_s = 1.313 \times 10^{-3}$ and $H_{\text{bias}} = 1.23 \times 10^4$ A/m.

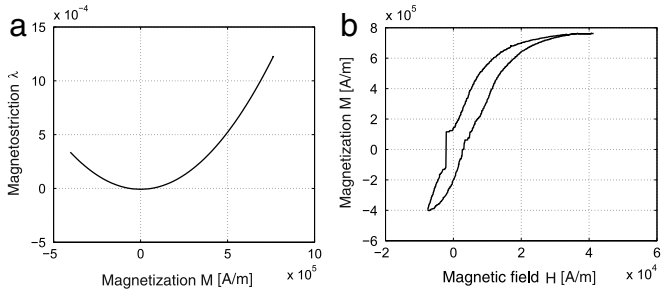

Fig. 9. Transformation from the butterfly to a simple closed curve. The ∨-unimodal relationship between M and λ obtained from (17) is shown in (a). (b) shows the simple hysteresis curve between the magnetic field H and magnetization M along the rod. A vertical jump due to unequal local minima of the butterfly map is visible at the point where the map crosses the H-axis.

Combining Definition 11 with (15) and (16), we transform the butterfly curve in Fig. 8 into a simple hysteresis curve between the magnetic field H and the magnetization along the rod M. Using the unimodal mapping (15), we obtain

$$M = \pm\sqrt{\frac{\lambda - b_1}{a_1}}. \tag{17}$$

The sign of M is chosen such that the H–M hysteresis curve is piecewise monotonically increasing, as dictated by the physics. The resulting plot of λ versus M is shown in Fig. 9(a). Eq. (16) is used to calculate the values of the magnetic field H corresponding to the input current. The resulting H–M hysteresis map is shown in Fig. 9(b). The vertical jump in the hysteresis map at the point where it crosses the x-axis is due to the fact that, because of measurement error, the two local minima of the butterfly map in Fig. 8 are not exactly equal. However, the experimental data approximately meet the assumptions of Theorems 9 and 10.

The piecewise monotone hysteresis map in Fig. 9(b) can be modeled with various operators, such as the Preisach operator and the Prandtl–Ishlinskii (PI) operator. As an example, we use the generalized PI operator given in Janaideh et al. (2008) and shown to accurately characterize hysteresis in magnetostrictive actuators. Since the generalized PI model has nonlocal memory, it can be used to model minor and major hysteresis loops and thus can easily be fit and inverted. The generalized PI model consists of generalized play operators that are defined by the input u, threshold r, and envelope function γ. As in Janaideh et al. (2008), we use the envelope function $\gamma = c_0 \tanh(c_1 u + c_2) + c_3$ and the density function $p(r) = \rho e^{-\tau r}$. We assume $r = \beta j$, where $j = 1, \ldots, 100$, and we minimize the error between the data and the model with a least squares optimization routine. The output of the optimization is summarized in Table 1.

Comparison of the output of the identified generalized PI model with parameters in Table 1 and experimental data in Fig. 9(b) is shown in Fig. 10(a). Using (14)–(16), we convert the output of the generalized PI model from Fig. 10(a) into a butterfly hysteresis curve. The comparison of this butterfly map and the experimentally measured data from Fig. 8 is shown in Fig. 10(b).

In the example above, we focused on only the major hysteresis loop. Ferromagnetic materials and many other smart materials demonstrate minor loops inside major loops. The same unimodal function used to reduce a major butterfly loop to a simple loop can be used to reduce minor butterfly loops without needing to choose different unimodal functions for the transformation of minor loops within a major loop. Conversely, applying a unimodal function to a piecewise monotone hysteresis operator that generates minor loops will lead to a hysteresis operator capable of generating minor butterfly loops.

Table 1
Identified parameters of the generalized PI model from the least squares optimization routine.

Parameter	Value	Parameter	Value
c_0	4.0904	c_1	0.777 m/A
c_2	−0.066	c_3	−0.269
ρ	4.640 A/m	τ	−0.191
q	11.961 A/m	β	1.139

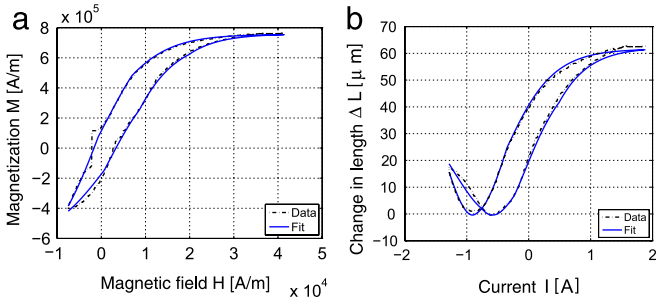

Fig. 10. Comparison of the experimental data and the simulated output of the PI model. (a) compares the experimental data shown in Fig. 9(b) and the output of the generalized PI model with parameters defined in Table 1. (b) compares the butterfly map obtained from experimental data in Fig. 8 and the butterfly map obtained by applying (15) and (16) to the output of the generalized PI model with parameters defined in Table 1.

5. Conclusions

We studied the relationship between simple and butterfly hysteresis maps and showed that they can be linked through unimodal functions in almost all cases. Depending on the context, such unimodal functions can be given by kinematics or underlying physics or can be chosen to facilitate analysis or control design. In particular, the proof of Theorem 9 provides a procedure to construct the simple hysteresis map given a butterfly and a chosen unimodal function. Two examples involving a nonlinear buckling system and a smart material actuator were used to illustrate the utility of the proposed framework in understanding, modeling, and compensating for butterfly hysteresis.

In the example of magnetostrictive hysteresis, the simple M–H hysteresis map obtained from the butterfly carries physical meaning (ferromagnetic hysteresis), and can in theory be experimentally validated using the measurement of M. However, in general, when we reduce a butterfly map to a simple hysteresis map for control purposes, the latter does not have to carry specific physical interpretation, and thus no validation is necessary.

Future work includes the extension of these results to include hysteretic unimodal maps and multibutterflies. The use of hysteretic unimodal maps may give more flexibility in the types of butterflies that can be obtained from a given simple hysteresis map and enable easier fits to experimental data in control applications.

References

Bernstein, D. S. (2007). Ivory ghost. *IEEE Control Systems Magazine*, *27*, 16–17.
Brokate, M., & Sprekels, J. (1996). *Hysteresis and phase transitions*. New York, NY: Springer.
Brown, W. F. (1966). *Magnetoelastic interactions*. Springer-Verlag.
Chen, X., Hisayama, T., & Su, C.-Y. (2009). Pseudo-inverse-based adaptive control for uncertain discrete time systems preceded by hysteresis. *Automatica*, *45*, 469–476.
Cross, R., Grinfeld, M., & Lamba, H. (2009). Hysteresis and economics: taking the economic past into account. *IEEE Control Systems Magazine*, *29*, 30–43.
Davi, F. (2001). On domain switching in deformable ferroelectrics, seen as continua with microstructure. *Zeitschrift fr Angewandte Mathematik und Physik*, *52*, 966–989.
Drinčić, B., & Bernstein, D.S. 2009. Why are some hysteresis loops shaped like a butterfly?. In *Proceedings of American control conference, St. Louis, MO* (pp. 3977–3982).

Ebine, N., & Ara, K. (1999). Magnetic measurement to evaluate material properties of ferromagnetic structural steels with planar coils. *IEEE Transaction on Magnetics*, *35*, 3928–3930.
Guillemin, V., & Pollack, A. (1974). *Differential topology*. Englewood Cliffs, NY: Prentice-Hall, Inc..
Iyer, R. V., & Tan, X. (2009). Control of hysteretic systems through inverse compensation. *IEEE Control Systems Magazine*, *29*, 83–99.
Janaideh, M.A., Mao, J., Rakheja, S., Xie, W., & Su, C.Y. 2008. Generalized Prandtl–Ishlinskii hysteresis model: hysteresis modeling and its inverse for compensation in smart actuators. In *Proceedings of IEEE conference on decision and control, Cancun, Mexico* (pp. 5182–5187).
Kuhnen, K. (2003). Modeling, identification and compensation of complex hysteretic nonlinearities: a modified Prandtl–Ishlinskii approach. *European Journal of Control*, *9*, 407–418.
Leang, K. K., Zou, Q., & Devasia, S. (2009). Feedforward control of piezoactuators in atomic force microscope systems. *IEEE Control Systems Magazine*, *29*, 70–82.
Li, J., & Weng, G. J. (2001). A micromechanics-based hysteresis model for ferroelectric ceramics. *Journal of Intelligent Material Systems and Structures*, *12*, 79–91.
Mayergoyz, I. D. (2003). *Mathematical models of hysteresis and their applications*. Amsterdam: Elsevier.
Oh, J., & Bernstein, D. S. (2005a). Semilinear Duhem model for rate-independent and rate-dependent hysteresis. *IEEE Transactions on Automatic Control*, *50*, 631–645.
Oh, J., & Bernstein, D.S. 2005b. Step-convergence analysis of nonlinear feedback hysteresis models. In *Proceedings of American control conference, Portland, OR* (pp. 697–702).
Oh, J., Drincic, B., & Bernstein, D. S. (2009). Nonlinear feedback models of hysteresis. *IEEE Control Systems Magazine*, *29*, 100–119.
Padthe, A. K., Chaturvedi, N. A., Bernstein, D. S., Bhat, S. P., & Waas, A. M. (2008). Feedback stabilization of snap-through buckling in a preloaded two-bar linkage with hysteresis. *International Journal of Non-Linear Mechanics*, *43*, 277–291.
Sahota, H. (2004). Simulation of butterfly loops in ferroelectric materials. *Continuum Mechanics and Thermodynamics*, *16*, 163–175.
Simitses, G. J. (1967). *An introduction to the elastic stability of structures*. Englewood Cliffs, NJ: Prentice Hall.
Tan, X. 2002. Control of smart actuators. *Ph.D. thesis*. MD: University of Maryland College Park.
Tan, X., & Baras, J. S. (2004). Modeling and control of hysteresis in magnetostrictive actuators. *Automatica*, *40*, 1469–1480.
Tan, X., & Iyer, R. V. (2009). Modeling and control of hysteresis. *IEEE Control Systems Magazine*, *29*, 26–29.
Visintin, A. (1994). *Differential models of hysteresis*. New York: Springer-Verlag.
Wang, Q., & Su, C.-Y. (2006). Robust adaptive control of a class of nonlinear systems including actuator hysteresis with Prandtl–Ishlinskii presentations. *Automatica*, *42*, 859–867.
Wen, C., & Zhou, J. (2007). Decentralized adaptive stabilization in the presence of unknown backlash-like hysteresis. *Automatica*, *43*, 426–440.

Bojana Drinčić is a Ph.D. Candidate at the University of Michigan. She received the Bachelor's degree in Aerospace Engineering in 1997 from the University of Texas at Austin and a Master's degree in Aerospace Engineering in 2009 from the University of Michigan. Her research interests include discontinuous systems and modeling of systems with hysteresis and friction.

Xiaobo Tan received the Bachelor's and Master's degrees in automatic control from Tsinghua University, Beijing, China, in 1995 and 1998, respectively, and the Ph.D. degree in electrical and computer engineering from the University of Maryland, College Park, in 2002.

From September 2002 to July 2004, he was a Research Associate with the Institute for Systems Research at the University of Maryland. In August 2004 he joined the Department of Electrical and Computer Engineering at Michigan State University (MSU) as an Assistant Professor, and founded the Smart Microsystems Laboratory. He has been an Associate Professor at MSU since July 2010. His current research interests include electroactive polymer sensors and actuators, biomimetic robotic fish, mobile sensing in aquatic environments, modeling and control of smart materials, and collaborative control of autonomous systems. Dr. Tan is also keen to integrate his research with educational and outreach activities, and currently leads an NSF-funded Research Experiences for Teachers (RET) Site on Bio-Inspired Technology and Systems (BITS) at MSU.

Dr. Tan has been an Associate Editor of Automatica since 2008. He served as the Program Chair for the 15th International Conference on Advanced Robotics (ICAR 2011), and was a guest editor of IEEE Control Systems Magazine for its February 2009 issue's special section on modeling and control of hysteresis. Dr. Tan received the NSF CAREER Award in 2006, the 2008 ASME DSCD Best Mechatronics Paper Award (with Yang Fang) in 2009, and the MSU Teacher–Scholar Award in 2010.

Dennis S. Bernstein is a professor in the Aerospace Engineering Department at the University of Michigan. He received the Ph.D. degree from the University of Michigan in 1982, and he became a faculty member at the University of Michigan in 1991. He is a Fellow of the IEEE. His research interests include system identification and adaptive control for aerospace applications.